

University of Nebraska - Lincoln  
**DigitalCommons@University of Nebraska - Lincoln**

---

Mechanical & Materials Engineering Faculty  
Publications

Mechanical & Materials Engineering, Department  
of

---

3-2019

# Interactions between dislocations and three-dimensional annealing twins in face centered cubic metals

Yanxiang Liang  
*University of Nebraska–Lincoln*

Xiaofang Yang  
*Chongqing University, yangxf@cqu.edu.cn*


Mingyu Gong  
*University of Nebraska–Lincoln, mgong4@unl.edu*

Guisen Liu  
*Shanghai Jiao Tong University*

Qing Liu  
*Chongqing University*

*See next page for additional authors*

Follow this and additional works at: <http://digitalcommons.unl.edu/mechengfacpub>

 Part of the [Mechanics of Materials Commons](#), [Nanoscience and Nanotechnology Commons](#), [Other Engineering Science and Materials Commons](#), and the [Other Mechanical Engineering Commons](#)

---

Liang, Yanxiang; Yang, Xiaofang; Gong, Mingyu; Liu, Guisen; Liu, Qing; and Wang, Jian, "Interactions between dislocations and three-dimensional annealing twins in face centered cubic metals" (2019). *Mechanical & Materials Engineering Faculty Publications*. 353. <http://digitalcommons.unl.edu/mechengfacpub/353>

This Article is brought to you for free and open access by the Mechanical & Materials Engineering, Department of at DigitalCommons@University of Nebraska - Lincoln. It has been accepted for inclusion in Mechanical & Materials Engineering Faculty Publications by an authorized administrator of DigitalCommons@University of Nebraska - Lincoln.

---

**Authors**

Yanxiang Liang, Xiaofang Yang, Mingyu Gong, Guisen Liu, Qing Liu, and Jian Wang

Published in *Computational Materials Science* 161 (2019), pp 371–378.

doi 10.1016/j.commatsci.2019.02.024

Submitted 15 January 2019; revised 17 February 2019; accepted 18 February 2019.

Copyright © 2019 Elsevier B.V. Used by permission.

# Interactions between dislocations and three-dimensional annealing twins in face centered cubic metals

Yanxiang Liang,<sup>1,2</sup> Xiaofang Yang,<sup>1</sup> Mingyu Gong,<sup>2</sup>  
Guisen Liu,<sup>3</sup> Qing Liu,<sup>1</sup> and Jian Wang<sup>2</sup>

1 International Joint Laboratory for Light Alloys (Ministry of Education),  
College of Materials Science and Engineering, Chongqing University,  
Chongqing 400044, China

2 Department of Mechanical & Materials Engineering, University of Nebraska–  
Lincoln, Lincoln, NE 68588 USA

3 State Key Lab of Metal Matrix Composites, School of Materials Science and  
Engineering, Shanghai Jiao Tong University, Shanghai 200240, China

*Corresponding authors* — X. Yang, yangxf@cqu.edu.cn ; J. Wang, jianwang@unl.edu

## Abstract

Annealing twins often form in metals with a face centered cubic structure during thermal and mechanical processing. Here, we conducted molecular dynamic (MD) simulations for copper and aluminum to study the interaction processes between  $\{111\}/2 <110>$  dislocations and a three-dimensional annealing twin. Twin boundaries are characterized with  $\Sigma 3\{111\}$  coherent twin boundaries (CTBs) and  $\Sigma 3\{112\}$  incoherent twin boundaries (ITBs). MD results revealed that dislocation-ITB interactions affect slip transmission for a dislocation crossing CTBs, facilitating the nucleation of Lomer dislocation.

**Keywords:** Annealing twin, Dislocation, Slip transmission, Molecular dynamics

## 1. Introduction

Annealing twins can form in metals with a face centered cubic (FCC) structure through thermal-mechanical processing. This phenomenon was firstly reported by the Carpenter and Tamura in 1926 [1]. Many models that address the formation of annealing twins can be classified into four groups,

**i)** the grain encounter model [2], **ii)** stacking fault model [3], **iii)** grain boundary dissociation model [4,5] and **iv)** growth accident model [6,7]. Annealing twins result in substantial evolution of microstructures and tailor mechanical properties in a large variety of metallic materials [1,8–11]. Twin boundaries (TBs) effectively strengthen materials by impeding dislocations motion and increase work-hardening capability [12]. For example, FCC-phase high entropy alloys generally exhibit low yield strength but superb ductility associated with slips and twinning [13,14]. Ming et al. realized a synchronized increase in strength and ductility of single FCC-phase CrFeCoNiMo alloy by developing hierarchical microstructure that comprises annealing nano-twins in recrystallized fine grains and stable dislocation walls in non-fully recrystallized fine grains [15]. Severe deformation at low temperature and followed annealing at room temperature led the formation of such hierarchical microstructures.

Twin boundaries associated with annealing twins in FCC materials are characterized with  $\Sigma 3\{1\ 1\ 1\}$  coherent twin boundaries (CTBs) and  $\Sigma 3\{1\ 1\ 2\}$  incoherent twin boundaries (ITBs) due to their low formation energies [16,17]. Many experimental observations and molecular dynamic simulations have been conducted to explore the interactions of dislocations with CTBs or ITBs individually [18–20].  $\Sigma 3\{1\ 1\ 1\}$  CTB is a strong barrier to slip transmission because of the discontinuity of slip systems [18,19,21]. Transmission mechanisms for dislocations vary with characters of incoming dislocations and local stress states in the vicinity of the boundary [22,23,24]. A screw dislocation can either cross slip onto the CTB plane or transmit onto the complementary  $\{1\ 1\ 1\}$  plane in the twin [19,20,25]. After slip transmission, no residual defect is left at the CTB [19,25]. A mixed dislocation under a shear stress parallel to the CTB plane glides from a  $\{1\ 1\ 1\}$  plane in matrix to a mirror  $\{1\ 1\ 1\}$  plane in the twin [18], but under biaxial loading parallel and/or normal to the CTB a mixed dislocation glides onto a  $\{1\ 0\ 0\}$  plane in the twin [26]. Differing from the case of screw dislocation, one Shockley partial is left at the CTB, causing the migration of the CTB [26]. In situ nanoindentation also suggested a multiplication mechanism for Shockley partial dislocations at CTBs through the dissociation of a full dislocation into and the reassembly of a Frank partial dislocation and a Shockley partial dislocation [27].  $\Sigma 3\{1\ 1\ 2\}$  ITBs associated with growth/annealing twin can be represented as a set of partial dislocations on every  $\{1\ 1\ 1\}$  plane [28]. The sum of these Burgers vectors in one triple unit equals zero. ITBs may dissociate into two tilt walls bounding a volume of 9R phase [29,30]. The separation of the two tilt walls is dependent on stacking fault energy and applied shear stress [29]. In situ indentation studies of nano-twinned Cu and Al have revealed slip transmission for dislocations across ITBs and formation of steps along ITBs [31–33].

Twins, however, are 3-dimensional domains. Practically all the work done on dislocation-twin interactions regards twins as two-dimensional entities, sectioned along the plane that contains the propagation and normal direction. In this article, we conducted molecular dynamic simulations to study the interaction processes of  $\{1\ 1\ 1\}/2<1\ 1\ 0>$  dislocations (screw-type and mixed-type) approaching a three-dimensional (3D) annealing twin. Cu with mediate stacking fault energy (SFE) and Al with high SFE are chosen for this study in order to explore the effect of SFE on interaction processes. The results revealed that dislocation-ITB interactions affect slip transmission for a dislocation across CTBs.

## 2. Atomistic simulations

**Fig. 1(a)** shows the possible slip systems in  $\bar{m}$  matrix and twin that are defined under the coordinate,  $\bar{x}$ -axis along  $[\bar{2}\ \bar{1}\ \bar{1}]_M$ ,  $\bar{y}$ -axis along  $[\bar{1}\ \bar{1}\ \bar{1}]_M$ , and  $\bar{z}$ -axis along  $[0\ \bar{1}\ \bar{1}]_M$ . On  $(\bar{1}\ \bar{1}\ \bar{1})_M$  plane, there are two mixed full dislocations ( $\mathbf{b}^I_1 = \frac{1}{2}[\bar{1}\ 0\ \bar{1}]_M$  and  $\mathbf{b}^{III}_1 = \frac{1}{2}[\bar{1}\ 1\ 0]_M$ ) and one screw full dislocation ( $\mathbf{b}^{II}_1 = \frac{1}{2}[0\ \bar{1}\ \bar{1}]_M$ ) as the line sense of dislocations is parallel to the  $\bar{z}$ -axis. Three full dislocations can be further written as the superposition of one edge partial dislocations ( $\mathbf{p}^{II}_1 = \frac{1}{6}[\bar{2}\ \bar{1}\ \bar{1}]_M$ ) and two mixed partial dislocations ( $\mathbf{p}^I_1 = \frac{1}{6}[\bar{1}\ 1\ \bar{2}]_M$  and  $\mathbf{p}^{III}_1 = \frac{1}{6}[\bar{1}\ \bar{2}\ \bar{1}]_M$ ). The  $(1\ 0\ 0)_T$  plane, as the candidate slip plane for dislocation transmission/transmutation, has 15.8x deviation from the  $(\bar{1}\ \bar{1}\ \bar{1})_M$  plane. Two full dislocations, an edge-type  $\mathbf{b}^I_2$  and a screw-type  $\mathbf{b}^{II}_2$ , can also glide on  $(1\ 0\ 0)_T$  plane. Besides  $(1\ 0\ 0)_T$  plane, full dislocation  $\mathbf{b}^{II}_1$  with screw character can cross slip onto  $(\bar{1}\ \bar{1}\ \bar{1})_T$  plane and the twin boundary plane ( $(\bar{1}\ 1\ 1)_M || (\bar{1}\ 1\ 1)_T$ ). It should be noted that  $\mathbf{b}^{II}_1$ ,  $-\mathbf{b}^{II}_2$ ,  $\mathbf{b}^{II}_3$ , and  $\mathbf{b}^{II}_4$  used in the following sections have the same Burgers vector.

Twin boundaries associated with annealing/growth twins in FCC metals have been systematically studied [34]. Three sets of tilt  $\Sigma 3$  GBs have been studied with respect to the tilt axis  $\langle 1\ 1\ 1 \rangle$ ,  $\langle 1\ 1\ 2 \rangle$ , and  $\langle 1\ 1\ 0 \rangle$ , respectively [34].  $\Sigma 3\ \{1\ 1\ 1\}$  CTB and  $\Sigma 3\{1\ 1\ 2\}$  ITBs are thermodynamically stable with low formation energy, which is consistent with TEM observation [17]. Moreover, atomic structures of ITBs vary with stacking fault energies (SFEs) [29,30]. Hereby, Cu and Al with mediate and high SFEs are taken as the model materials. The simulation models start with a  $26 \times 46 \times 40$  nm Cu single crystal and a  $29 \times 52 \times 46$  nm Al single crystal. The coordinate is  $\bar{x}$ -axis along  $[\bar{2}\ \bar{1}\ \bar{1}]_M$ ,  $\bar{y}$ -axis along  $[\bar{1}\ \bar{1}\ \bar{1}]_M$ , and  $\bar{z}$ -axis along  $[0\ \bar{1}\ \bar{1}]_M$ . A  $15 \times 50 \times 5$  nm region in the single model is selected and rotated about the  $\bar{x}$ -axis for  $180^\circ$ . A twinned domain is created, as shown in Fig. 1(b). The initial twin boundaries comprise  $\Sigma 3\ \{1\ 1\ 1\}$  CTB and  $\Sigma 3\{1\ 1\ 2\}$  ITBs.

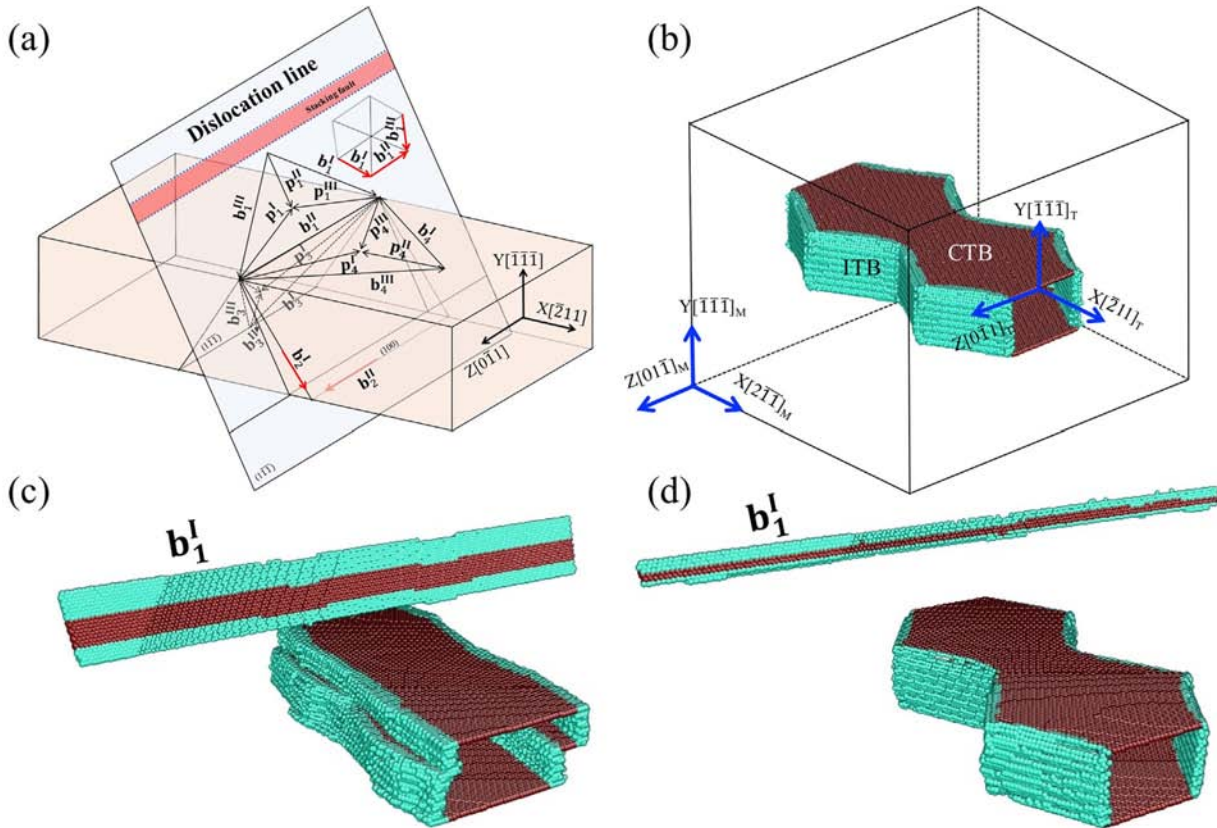


**Fig. 1.** (a) A schematic 3D annealing twin and the available slip systems. The blue dashed lines and red stripe denote two Shockley partial dislocations and stacking fault region. The dislocation line is initially along the z-axis. (b) The initial 3D twin morphology, showing ITBs (cyan) and CTBs (red). Atomic configurations of initial simulation models, showing a 3D annealing twin and an extended  $60^\circ$  mixed dislocation in Cu (c), and a 3D annealing twin and an extended  $60^\circ$  mixed dislocation in Al (d).

Corresponding to the crystallography of the twin, two mixed full dislocations  $b_1^I$  and  $b_1^{II}$  will result similar interaction processes with the twin though they have opposite screw components. In the following simulations, we studied the interaction process between a mixed dislocation  $b^I$  as well as a screw dislocation  $b^{II}$  and the 3D twin. The introduction of a dislocation into the twined model is accomplished by the application of anisotropic Barnett-Lothe solutions for the displacement field of a dislocation in the bi-crystal [35]. We initially introduce a dislocation on  $(1\bar{1}\bar{1})_M$  plane at 4 nm from the upper CTB. With periodic boundary conditions along x- and z-directions and fixed boundary condition in y-direction, the dislocation-twin structures are then relaxed at 0 K until the maximum force acting on each atom is less than 5 pN. During relaxation, the embedded atom method potentials for

Cu [36] and Al [37] are employed. These potentials have shown to provide reliable results in studies of energetics and kinetics of surfaces, defects, interfaces, and crystal growth [36,37]. The relaxed structures for Cu and Al are shown in Fig. 1(c) and (d). The wider dislocation core is found for Cu due to its low SFE. The irregular-shaped twin for Cu is attributed to high mobility of ITBs in Cu [16]. The relaxed structures are then subjected to constant deformation rate at 5 K. More simulation details will be described with respect to each simulation case.

### 3. Dislocation-3D twin interactions

#### 3.1. A screw dislocation-3D twin interactions

**Figs. 2(a) and 3(a)** show the relaxed structures containing the screw dislocation  $\mathbf{b}_1^{\parallel}$  and the 3D twin in Cu and Al, respectively.  $\mathbf{b}_1^{\parallel}$  splits into two mixed partial dislocations  $-\mathbf{p}_1^{\parallel}$  and  $\mathbf{p}_1^{\parallel}$ . In Cu with low SFE, the separation between the two partials are larger than that in Al. Besides the cross-slip of the  $\mathbf{b}_1^{\parallel}$

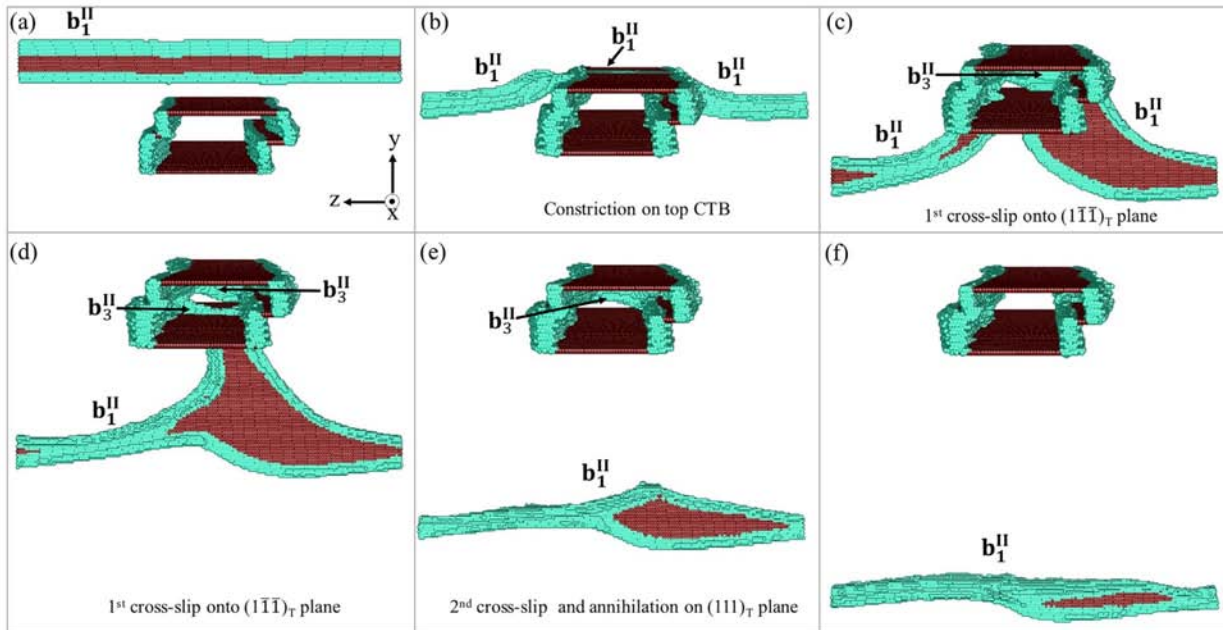


**Fig. 2.** (a) Initial 3D atomic configuration showing a 3D annealing twin and a pure screw dislocation  $\mathbf{b}_1^{\parallel}$ . (b) and (c)  $\mathbf{b}_1^{\parallel}$  crosses the upper CTB into the twin, and a new dislocation  $\mathbf{b}_3^{\parallel}$  dislocation nucleates. (d)  $\mathbf{b}_1^{\parallel}$  crosses the lower CTB into the twin and a new dislocation  $\mathbf{b}_3^{\parallel}$  nucleates in the twin. (e) Annihilation of the two  $\mathbf{b}_3^{\parallel}$  dislocations by cross-slip onto  $(111)_T$  plane in the twin. (f) An annealing twin without steps left on CTBs after  $\mathbf{b}_1^{\parallel}$  dislocation loops the 3D twin.

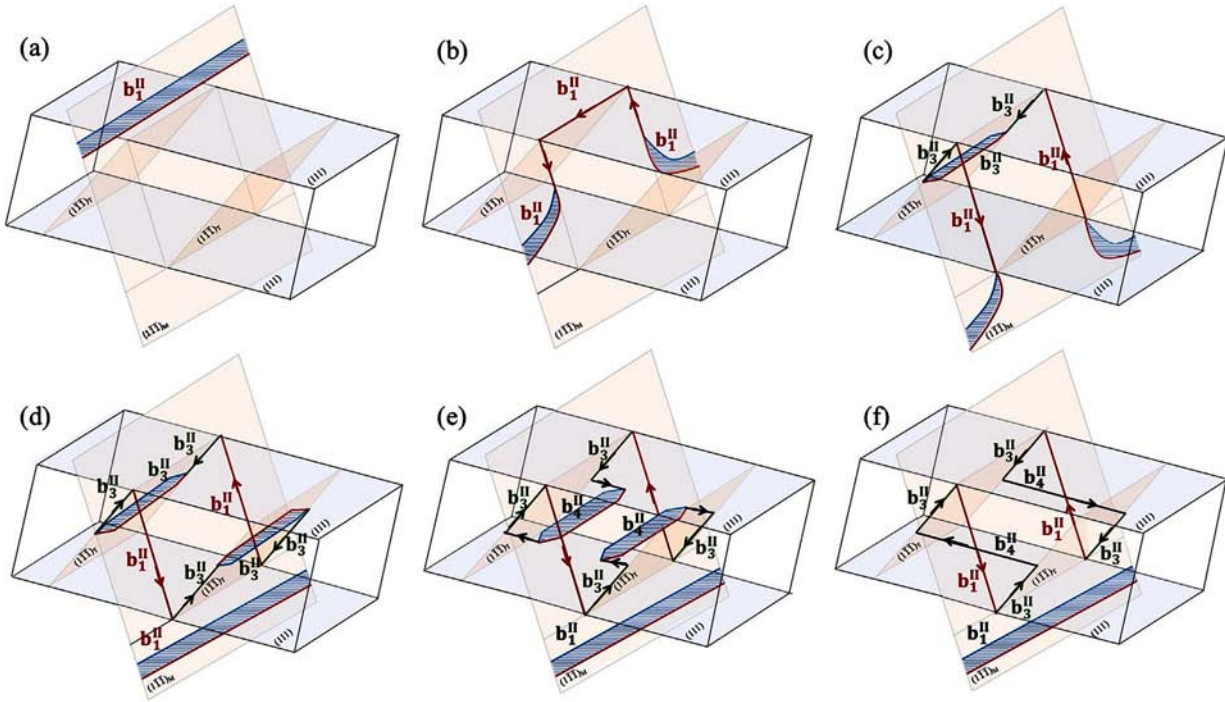


**Fig. 3.** Schematics of the interaction between a screw dislocation  $\mathbf{b}_1^{\parallel}$  and a 3D annealing twin in Cu. **(a)** Initial 3D annealing twin and a core-extended pure screw dislocation  $\mathbf{b}_1^{\parallel}$ . **(b)**  $\mathbf{b}_1^{\parallel}$  starts looping over the 3D twin. **(c)** Transmutation of  $\mathbf{b}_1^{\parallel}$  across the upper CTB into the twin domain. **(d)** Transmutation of  $\mathbf{b}_1^{\parallel}$  across the lower CTB into the twin. **(e)** Two  $\mathbf{b}_3^{\parallel}$  dislocations cross slip onto  $(1\ 1\ 1)_T$  plane and then dislocation annihilation takes place inside the twin. **(f)**  $\mathbf{b}_1^{\parallel}$  glides on initial slip plane, leaving dislocation loops on ITBs. The arrow on dislocation line represents the dislocation line vector.

onto  $(1\ 0\ 0)_T$  plane and  $(1\ \bar{1}\ \bar{1})_T$  plane,  $\mathbf{b}_1^{\parallel}$  dislocation can also cross slip onto the twin boundary plane with two partials  $\mathbf{p}_4^{\parallel}$  and  $-\mathbf{p}_4^{\parallel}$ . In order to activate different cross-slip processes, we applied two representative loadings, 1st loading (constant deformation rate  $\dot{\mathbf{F}}_1$ ) and 2nd loading ( $\dot{\mathbf{F}}_2$ ),

$$\dot{\mathbf{F}}_1 = \dot{\gamma}_0 \begin{pmatrix} 0 & 0 & 0 \\ 0 & 0 & 0 \\ -1 & 0 & 0 \end{pmatrix} \quad (1)$$

$$\dot{\mathbf{F}}_2 = \dot{\gamma}_0 \begin{pmatrix} 0 & -1 & 0 \\ 0 & 0 & 0 \\ -1 & 0 & 0 \end{pmatrix} \quad (2)$$

where  $\dot{\gamma}_0 = 3 \times 10^8\ \text{s}^{-1}$ . When deformation gradients are equal to 1% ( $\mathbf{F}_1$  and  $\mathbf{F}_2$ ), we estimated the stress field  $\sigma$  at the deformation gradient, and then



calculated Peach-Koehler force  $\vec{F} = (\sigma \cdot \vec{b}) \times d\vec{l}$ , where  $\sigma$  is local stress,  $\vec{b}$  is Burgers vector and  $d\vec{l}$  is line direction. The RSS is calculated to be  $F_g/|b|$ , where  $F_g$  is the gliding force. The RSS in Cu/Al is 2.83/1.61 GPa for  $\mathbf{b}^{\text{II}}_1$  on  $(1\bar{1}\bar{1})_M$  and for  $\mathbf{b}^{\text{II}}_1$  on  $(1\bar{1}\bar{1})_T$  plane, zero for  $\mathbf{b}^{\text{II}}_4$  on the twin boundary plane and 2.44/1.33 GPa RSS for  $\mathbf{b}^{\text{II}}_2$  on  $(100)_T$  plane. Although the RSS for  $\mathbf{b}^{\text{II}}_4$  on the twin boundary plane is equal to zero, the RSS for the two partials on twin plane is different.  $\dot{\mathbf{F}}_1$  generates zero RSS for  $\mathbf{p}^{\text{I}}_4$  and  $-\mathbf{p}^{\text{III}}_4$  on the twin boundary plane but  $\dot{\mathbf{F}}_2$  results in 591.5/463.0 MPa RSS for  $\mathbf{p}^{\text{I}}_4$  and  $-591.5/-463.0$  MPa RSS for  $-\mathbf{p}^{\text{III}}_4$  on the twin boundary plane. Therefore,  $\dot{\mathbf{F}}_2$  favors the cross-slip for  $\mathbf{b}^{\text{II}}_1$  onto the twin boundary plane because of non-zero RSS for  $\mathbf{p}^{\text{I}}_4$  and  $-\mathbf{p}^{\text{III}}_4$ . Here, it should be mentioned that such prediction does not take the role of ITBs into account.

### 3.1.1. Interaction process under the 1st loading

Under the 1st loading, cross-slips of  $\mathbf{b}^{\text{II}}_1$  onto  $(100)_T$  or  $(1\bar{1}\bar{1})_T$  planes during the interaction are expected. In Cu,  $\mathbf{b}^{\text{II}}_1$  passes the twin without the generation of additional defects at the CTBs by dislocation looping mechanisms. **Fig. 2** shows the interaction process and Fig. 3 schematically explains the process. Under loading,  $\mathbf{b}^{\text{II}}_1$  with planar-extended core moves towards the twin (Figs. 2(a) and 3(a)). Figs. 2(b) and 3(b) shows the snapshots when  $\mathbf{b}^{\text{II}}_1$  reaches the upper CTB. The part of  $\mathbf{b}^{\text{II}}_1$  that touches the upper CTB exhibits a condensed core while the other part remains a planar-extended core. Driven by loading, looping of  $\mathbf{b}^{\text{II}}_1$  over the twin is observed (Fig. 2(c) and (d)), forming  $\mathbf{b}^{\text{II}}_1$  dislocation on the lower CTB with opposite line vector comparing to  $\mathbf{b}^{\text{II}}_1$  dislocation on the upper CTB. During looping, 1st cross-slip of  $\mathbf{b}^{\text{II}}_1$  (Figs. 2(c) and 3(c)) from the upper CTB and 2nd cross-slip of  $\mathbf{b}^{\text{II}}_1$  from the lower CTB (Figs. 2(d) and 3(d)) onto two parallel  $(1\bar{1}\bar{1})_T$  planes occur. Two dislocations  $\mathbf{b}^{\text{II}}_3$  nucleate and glide on  $(1\bar{1}\bar{1})_T$  planes. With further glide of the two  $\mathbf{b}^{\text{II}}_3$  on  $(1\bar{1}\bar{1})_T$  planes to the same height in y-direction, the attraction between them facilitate the 2nd cross-slips (Figs. 2(e) and 3(e)) of the two  $\mathbf{b}^{\text{II}}_3$  dislocations onto the same  $(1\bar{1}\bar{1})_T$  plane. Then, dislocation annihilation takes place since two dislocations with the opposite line sense and the same Burgers vector. In the final structure (Figs. 2(f) and 3(f)), four  $\mathbf{b}^{\text{II}}_1$  loops are left on ITBs. In principle, annihilation can also occur on  $(1\bar{1}\bar{1})_T$  plane, if the incoming dislocation on the top CTB crosses slip onto the  $(1\bar{1}\bar{1})_T$  plane, the incoming dislocation from the bottom CTB transfers into the twin and glides into the top CTB.

In Al, as shown in **Fig. 4**, only looping of  $\mathbf{b}^{\text{II}}_1$  over the twin is observed while the cross-slips and annihilation don't happen. Under loading,  $\mathbf{b}^{\text{II}}_1$  with a condensed core moves towards the twin (Fig. 4(a) and (a')) and is obstructed by the upper CTB (Fig. 4(b) and (b')). Then,  $\mathbf{b}^{\text{II}}_1$  forms on the lower CTB after looping. Differing from the case in Cu, CTBs show strong obstruction to two  $\mathbf{b}^{\text{II}}_1$  dislocations, making cross-slips harder to happen (Fig. 4(c) and (c')).

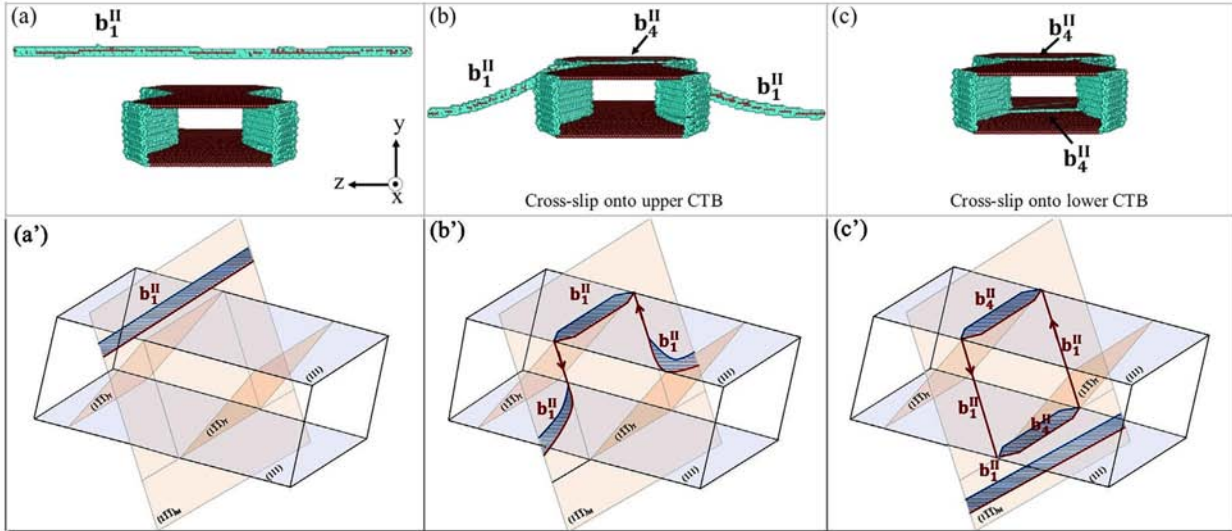


**Fig. 4.** Interaction between a pure screw dislocation and a 3D annealing twin in Al. **(a)** and **(a')** Initial 3D atomic configuration containing an annealing twin and a pure screw dislocation  $\mathbf{b}_1^{\text{II}}$ . **(b)** and **(b')** Cross-slip of  $\mathbf{b}_1^{\text{II}}$  from matrix onto the upper CTB, **(c)** Dislocations structures around the 3D twin after the looping of  $\mathbf{b}_1^{\text{II}}$  over the 3D twin.

### 3.1.2. Interaction process under the 2nd loading

Under the 2nd loading, cross-slips of  $\mathbf{b}_1^{\text{II}}$  onto  $(1\ 0\ 0)_T$  or  $(1\ \bar{1}\ \bar{1})_T$  planes and glide of  $\mathbf{p}_4^{\text{I}}$  and  $-\mathbf{p}_4^{\text{III}}$  on the twin boundary plane during the interaction are possible. In Cu, looping process is similar to that described in Figs. 2 and 3, leaving two  $\mathbf{b}_1^{\text{II}}$  dislocations along the intersection line between  $(1\ \bar{1}\ \bar{1})_M$  and the twin boundary plane. Instead of the cross-slips onto  $(1\ 0\ 0)_T$  or  $(1\ \bar{1}\ \bar{1})_T$  planes,  $\mathbf{b}_1^{\text{II}}$  dissociates into  $\mathbf{p}_4^{\text{I}}$  and  $-\mathbf{p}_4^{\text{III}}$  on the upper CTB and lower CTB planes. With the opposite RSS associated with  $\mathbf{p}_4^{\text{I}}$  and  $-\mathbf{p}_4^{\text{III}}$  on the twin boundary plane,  $\mathbf{p}_4^{\text{I}}$  and  $-\mathbf{p}_4^{\text{III}}$  glide in the opposite direction, thickening the twin by one layer (Fig. 5(a and b)). Despite the interaction process differs, the final structure under the 2nd loading is similar to that under the 1st loading (Fig. 4(c)).

In Al, **Fig. 5(c–g')** reveals some features different from previous simulations [19,20] except the dislocation looping over the 3D twin. During looping (Fig. 5(d) and (e)), part of the condensed-core  $\mathbf{b}_1^{\text{II}}$  dislocation on the upper CTB crosses slip onto the  $(1\ 0\ 0)_T$  plane from the ITBs as show in Fig. 5(e) and (e'). Wang et al. reported such a similar process in twinned nanowire where free surface favors such a cross-slip [26]. Due to the  $15.8^\circ$  deviation angle between the glide plane  $(1\ \bar{1}\ \bar{1})_M$  (on which  $\mathbf{b}_1^{\text{II}}$  glides) and the glide plane  $(1\ 0\ 0)_T$  (on which  $-\mathbf{b}_2^{\text{II}}$  glides), a dislocation segment created on ITBs (marked by red solid line in Fig. 5(e')) connects  $\mathbf{b}_1^{\text{II}}$  on  $(1\ \bar{1}\ \bar{1})_M$  and  $-\mathbf{b}_2^{\text{II}}$  on

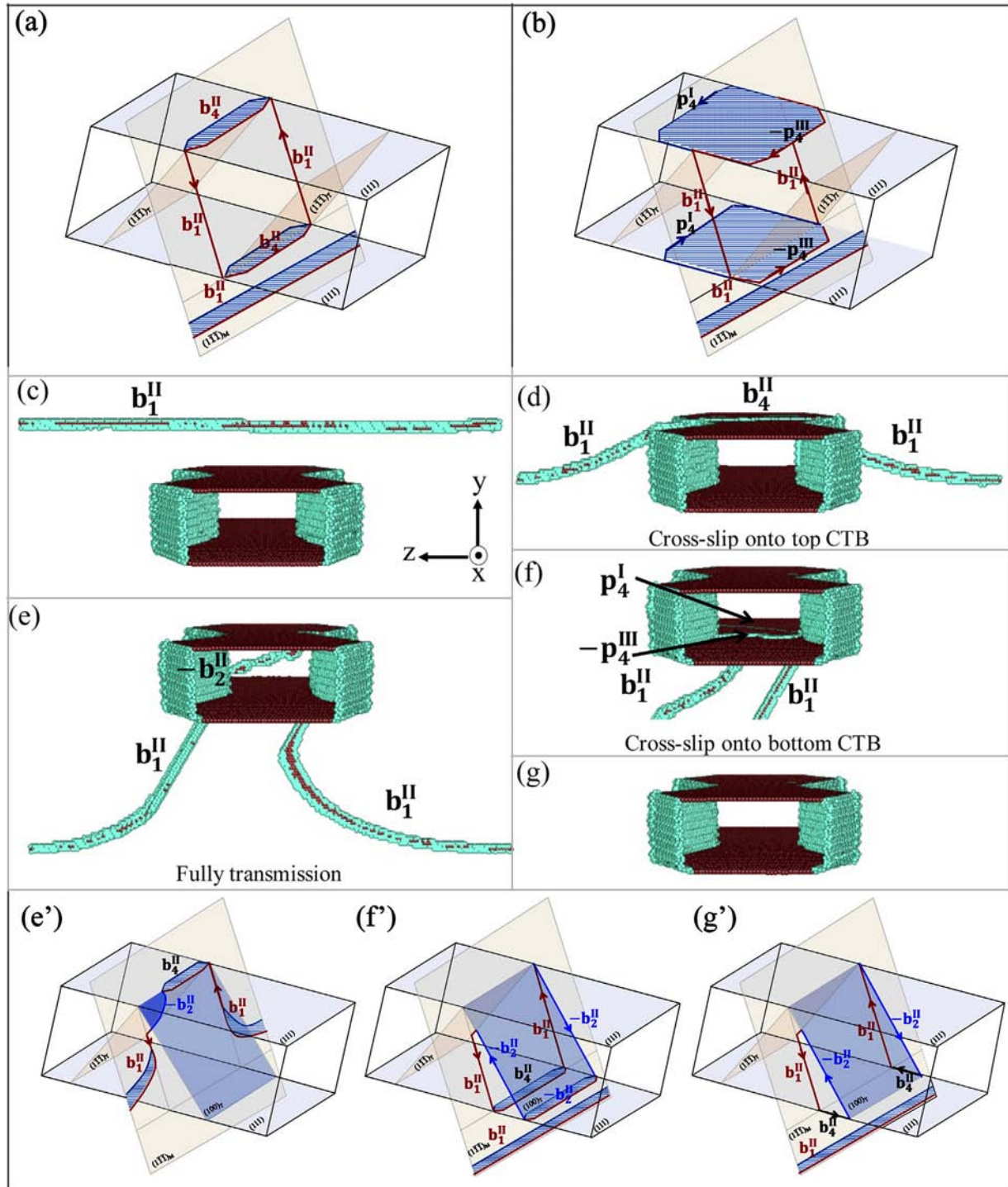


**Fig. 5.** Interaction between a pure screw dislocation  $\mathbf{b}_1^{\text{II}}$  and a 3D twin in Cu (a–b) and Al (c–g). In Cu, (a) A dislocation loop on 3D twin boundaries in Cu and (b) A screw dislocation  $\mathbf{b}_1^{\text{II}}$  dissociates onto CTBs, thickening the twin by one atom layer. In Al, (c) Initial 3D atomic configuration containing an annealing twin and a pure screw dislocation  $\mathbf{b}_1^{\text{II}}$ , (d)  $\mathbf{b}_1^{\text{II}}$  cross-slip onto the upper CTB, (e)  $\mathbf{b}_1^{\text{II}}$  transmission into the twin, (f)  $-\mathbf{b}_2^{\text{II}}$  cross-slip onto lower CTB, and (g) Perfect CTB with steps free after annihilation of the  $-\mathbf{b}_2^{\text{II}}$  and  $\mathbf{b}_4^{\text{II}}$ . (e'–g') Schematic of nucleation and glide of a dislocation on (1 0 0)<sub>γ</sub> plane from the CTB-ITB corner and the annihilation of dislocations on the lower CTB.

$(1\ 0\ 0)_T$  planes. Since the Burgers vector of this segment is not lying on the ITBs, the segment does not glide on the ITB. When  $-\mathbf{b}^{\text{II}}_2$  on  $(1\ 0\ 0)_T$  plane reaches the lower CTB (Fig. 5(f) and (f')), it dissociates into  $\mathbf{p}^{\text{I}}_4$  and  $-\mathbf{p}^{\text{III}}_4$ . In Fig. 5(g) and (g'),  $\mathbf{p}^{\text{I}}_4$  and  $-\mathbf{p}^{\text{III}}_4$  are cancelled by  $\mathbf{p}^{\text{I}}_4$  and  $-\mathbf{p}^{\text{III}}_4$  that are dissociated from  $\mathbf{b}^{\text{II}}_4$  ( $\mathbf{b}^{\text{II}}_1$ ) on the lower CTB. In the final structure, two dislocation loops are left on ITBs while the CTBs are defect free. In general, the  $(1\ 0\ 0)$  plane is not a common slip plane, but slip on  $(1\ 0\ 0)$  plane happens under specific local stress states. In our simulation, the cross-slip on  $(1\ 0\ 0)$  plane is attributed to high Schmid factor on  $(1\ 0\ 0)_T$  plane. Furthermore, the ITB provides a pathway for dislocation climb, realigning the dislocation line on the  $(1\ 0\ 0)_T$  plane. Under the 1st loading, we only observed cross-slip onto  $(1\ 1\ 1)_T$  plane in Cu and  $(1\ 1\ 1)_T$  plane in Al. This is because the stress field does not favor the climb of the dislocation on ITB.

### 3.2. A 60° mixed dislocation-3D twin interactions

Figs. 6(a) and 7(a) show the relaxed structures containing the mixed full dislocation  $\mathbf{b}^{\text{I}}_1$  and the 3D twin in Cu and Al, respectively. In both Cu and Al,  $\mathbf{b}^{\text{I}}_1$  dislocation splits into an edge  $\mathbf{p}^{\text{II}}_1$  and a mixed  $-\mathbf{p}^{\text{III}}_1$  partial dislocations. Affected by SFE,  $\mathbf{b}^{\text{I}}_1$  has a wider core in Cu and a condensed core in Al. With the mixed character,  $\mathbf{b}^{\text{I}}_1$  cannot cross slip onto other planes. The 3rd loading with the constant deformation rate  $\mathbf{F}_3$

$$\dot{\mathbf{F}}_3 = \dot{\gamma}_0 \begin{pmatrix} 0 & -1 & 0 \\ 0 & 0 & 0 \\ -1 & 0 & 0 \end{pmatrix} \quad (3)$$

is applied to the relaxed structures.  $\dot{\gamma}_0 = 3 \times 10^8 \text{ s}^{-1}$ . Under the loading, the RSSes in Cu/Al (estimated at 1% strain) are  $\underline{2.71/1.45}$ ,  $\underline{2.71/1.45}$ ,  $0.55/0.06$  and  $3.10/1.56$  GPa associated with  $\mathbf{b}^{\text{I}}_1$  on  $(1\ 1\ 1)_M$ ,  $-\mathbf{b}^{\text{I}}_3$  on  $(1\ 1\ 1)_T$  plane,  $\mathbf{b}^{\text{I}}_4$  on the twin boundary plane and  $-\mathbf{b}^{\text{I}}_2$  on  $(1\ 0\ 0)_T$  plane, respectively. Transmission, transmutation and dissociation of dislocations on  $(1\ \bar{1}\ \bar{1})_T$ ,  $(1\ 0\ 0)_T$  and twin boundary plane are possible. Dislocation transmutation is similar to dislocation transformation, meaning that a new dislocation nucleates at interface when an incoming dislocation enters the interface. As result, shear associated with the incoming dislocation is partially or fully transformed in the adjacent grain across the interface. In our MD simulations, the interaction between a dislocation and twin boundary is accomplished through nucleation and emission of another dislocation in the twin. The two dislocations may or may not have the same character. In FCC, both experiments and molecular dynamic simulations have demonstrated the possibility of a dislocation gliding on  $\{1\ 0\ 0\}$  plane [26,38,39]. Because the glide of dislocations on  $\{1\ 0\ 0\}$  plane is hard, the RSS of  $\mathbf{b}^{\text{I}}_2$  on  $(1\ 0\ 0)_T$  plane is designed

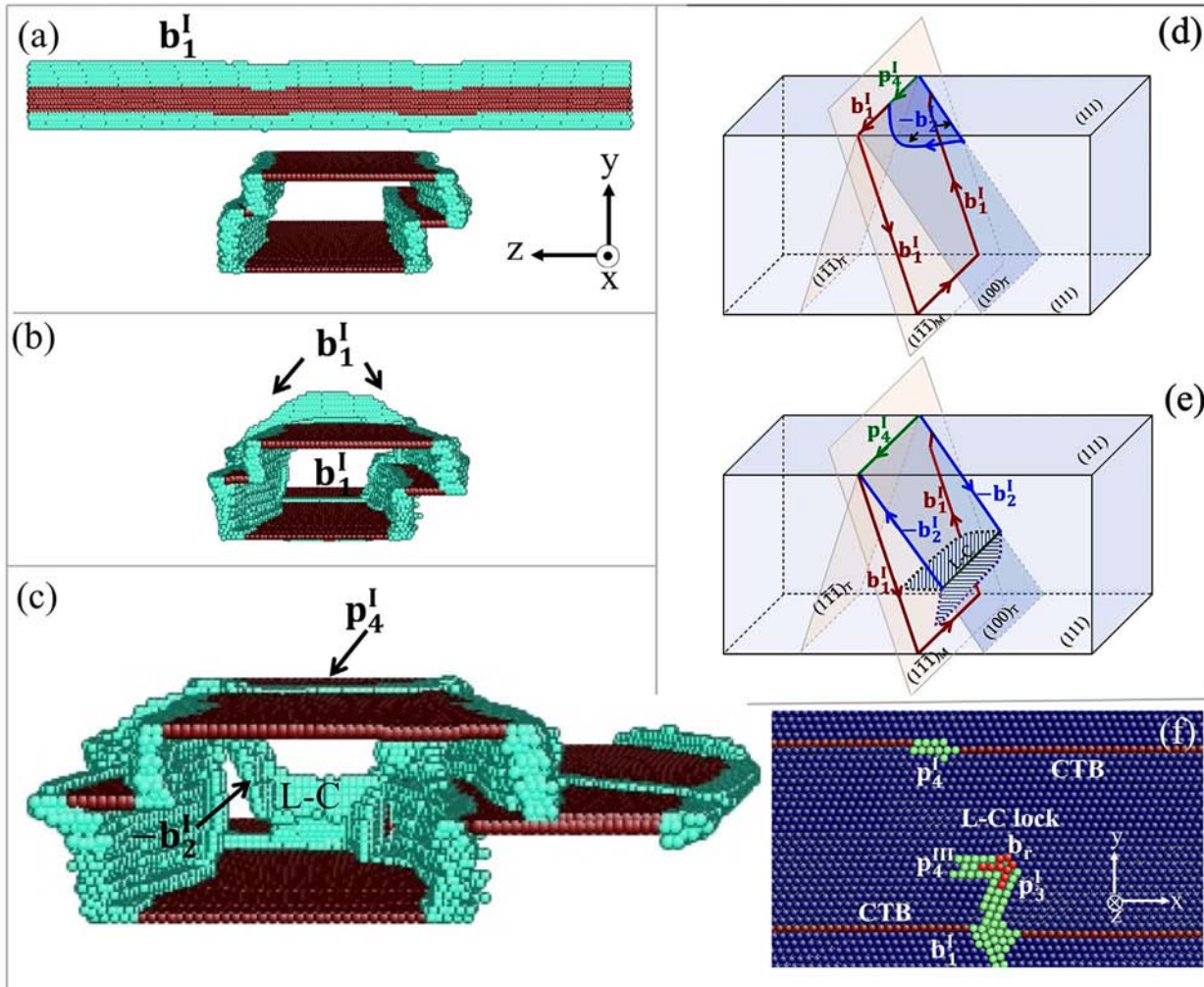


**Fig. 6.** Interaction between a mixed dislocation  $\mathbf{b}_1^I$  and a 3D twin in Cu. **(a)** Initial 3D atomic configuration containing a 3D twin and a  $60^\circ$  mixed dislocation  $\mathbf{b}_1^I$ . **(b)** Dislocation loops the 3D twin. **(c)** and **(d)** The nucleation and glide of a Lomer dislocation  $-\mathbf{b}_2^I$  on  $(1\ 0\ 0)_T$  plane in the twin. **(e)** The dissociation of a Lomer dislocation  $-\mathbf{b}_2^I$  on two  $\{1\ 1\ 1\}$  planes, forming a Lomer-Cottrell lock. **(f)** Atomic configuration showing the Lomer-Cottrell lock and Shockley partial dislocations on the upper CTB.

to be the largest among all possible slip systems. Figs. 6 and 7 describe the interaction between  $\mathbf{b}_{1\ i}$  and the 3D twin in Cu and Al. In both material systems, looping of  $\mathbf{b}_1^I$  over the twin (Figs. 6(c) and 7(c)) is always observed.

In Cu, as shown in Fig. 6(c), a Lomer dislocation  $-\mathbf{b}_2^I$  nucleates and glides on  $(1\ 0\ 0)_T$ , leaving a partial dislocation  $\mathbf{p}_4^I$  on the upper twin boundary. Reaction can be described by  $\mathbf{b}_1^I \rightarrow -\mathbf{b}_2^I + \mathbf{p}_4^I$ . The Lomer dislocation  $-\mathbf{b}_2^I$  then dissociates into partials  $\mathbf{p}_3^I$  on  $(1\ \bar{1}\ 1)_T$  plane,  $\mathbf{p}_4^{II}$  on  $(1\ 1\ 1)_T$  plane and a Stairrod dislocation  $b_r$ . The dissociation is energetically favorable and facilitated

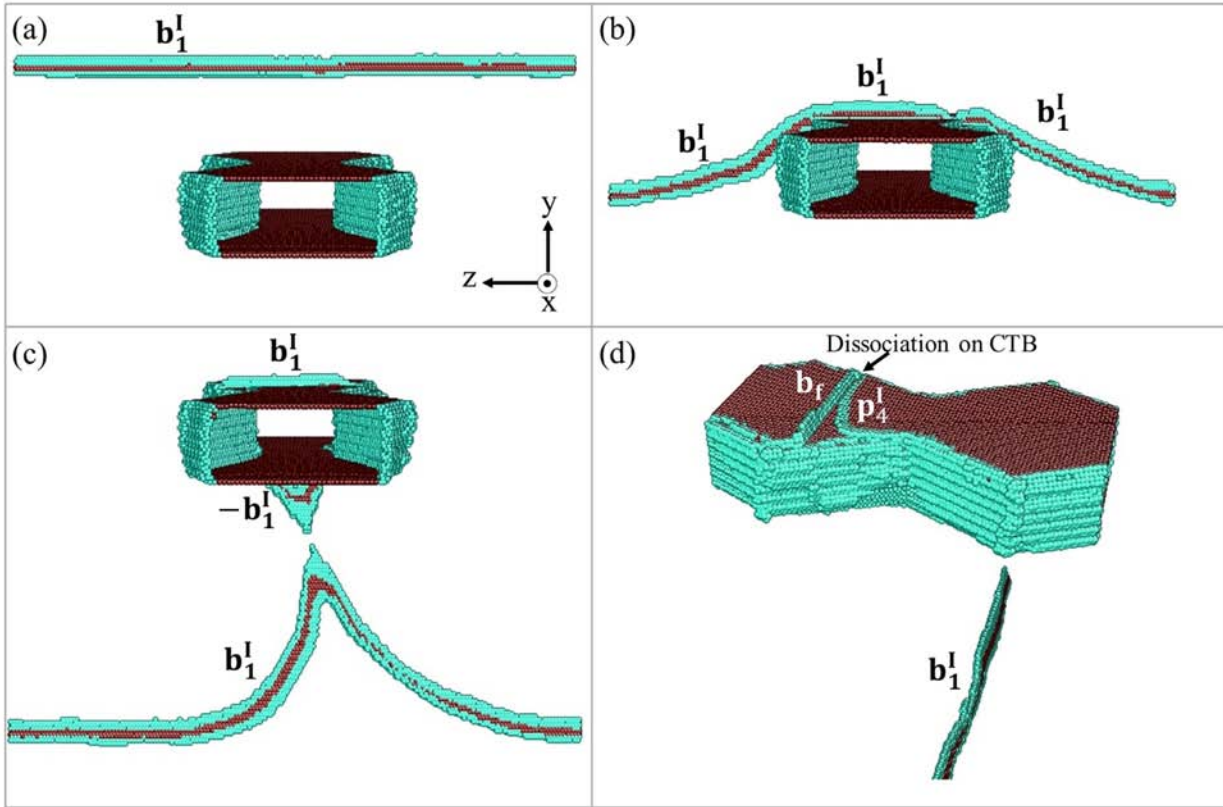


**Fig. 7.** Interaction between a mixed dislocation  $\mathbf{b}_1^I$  and a 3D twin in Al. **(a)** Initial 3D atomic configuration containing a 3D annealing twin and a mixed dislocation  $\mathbf{b}_1^I$ . **(b)**  $\mathbf{b}_1^I$  touches on the upper CTB. **(c)**  $\mathbf{b}_1^I$  dislocation loops the 3D twin, leaving a dislocation loop on twin boundaries. **(d)** The dissociation of  $\mathbf{b}_1^I$  onto a Frank partial and a Shockley partial on the upper CTB.

by the local stress associated with  $-\mathbf{b}_1^I$  on the lower CTB. The dissociation is described by the following reaction  $-\mathbf{b}_1^I \rightarrow \mathbf{p}_3^I + \mathbf{p}_4^I + \mathbf{b}_f$ .  $\mathbf{p}_3^I$ ,  $\mathbf{p}_4^I$  and  $\mathbf{b}_f$  form a Lomer-Cottrell (L-C) lock, as shown in Fig. 6(f). The L-C lock together with  $\mathbf{b}_1^I$  on ITBs will contribute to the hardening of the material. Slip transmission from  $(1\ 1\ 1)_M$  to  $(1\ 0\ 0)_T$  is difficult in general. It was reported in nanowires where free surface favors the nucleation of the dislocation on  $\{1\ 0\ 0\}$  plane [26]. In our case, there is no free surface, but the dislocation loops the twin. The dislocation segment on ITB can climb, realigning the dislocation line from  $(1\ 1\ 1)_M$  to  $(1\ 0\ 0)_T$  plane, which facilitates slip transmission from  $(1\ 1\ 1)_M$  to  $(1\ 0\ 0)_T$ . During looping process in Al, on the upper CTB, the dissociation of  $\mathbf{b}_1^I$  (Fig. 7(b)) into  $\mathbf{p}_4^I$  on the twin boundary plane and a sessile Frank partial dislocation  $\mathbf{b}_f$  with Burgers vector  $\frac{1}{3}[1\ 1\ 1]_M$ .

$\mathbf{p}_4^I$  glides on the twin boundary, thickening the twin by one atomic layer (Fig. 7(c)). In Fig. 7(d), final structure contains sessile Frank partial dislocations on CTBs and  $\mathbf{b}_1^I$  on ITBs. During the interaction between  $\mathbf{b}_1^I$  dislocation and twin, sessile L-C lock inside twin in Cu and Frank partial dislocation on CTB in Al are generated. On lateral side of the twin,  $\mathbf{b}_1^I$  piles up on ITBs.

#### 4. Conclusion

We conducted MD simulations of the interaction between the dislocations and a 3D annealing twin in copper and aluminum. The lateral boundaries of annealing twins are characterized by ITBs that are composed of an array of Shockley partial dislocations. The migration of ITBs during deformation was observed in all simulation cases of Cu, but was not apparent in Al. These results implied the irregular shape for annealing twins might in Cu and the regular shape for annealing twins in Al, which is consistent with previous study [16,29].

When a screw dislocation moves towards the 3D annealing twin, several scenarios may happen. For Cu, when a screw dislocation enters the twin boundaries by external stress, the dislocation is temporarily blocked by twin boundaries. As the deformation continues, the screw dislocation can transmit across both upper and lower CTBs and then annihilate inside the twin by cross-slips, depending on the applied shear stress. For Al, a screw dislocation may cross slip onto CTBs or transmit into  $(1\ 0\ 0)_T$  in the twin.

When a  $60^\circ$  mixed dislocation interacts a 3D twin, a  $\frac{1}{2}\langle 1\ 1\ 0 \rangle$  dislocation generates and glides on a  $(1\ 0\ 0)$  plane and leaves a glissile dislocation of Burgers vector  $\frac{1}{6}\langle 1\ 1\ 2 \rangle$  on the twin boundary in the case of Cu. Anomalous dislocation  $\frac{1}{2}\langle 1\ 1\ 0 \rangle$  on  $(1\ 0\ 0)_T$  plane can dissociate into a L-C lock. For Al, a dislocation loop will leave on twin boundaries. Dislocation segments on CTBs can dissociate into a Shockley partial dislocation and a Frank partial dislocation on CTBs.

During the interaction between a screw dislocation and twin under the 2nd loading in Al as well as that between a mixed dislocation and twin under the 3rd loading in Cu, the nucleation of a Lomer dislocation on  $(1\ 0\ 0)_T$  plane takes place at the CTB-ITB corner. In these cases, local stress associated with ITBs together with high RSS for dislocations on  $(1\ 0\ 0)_T$  plane facilitate the nucleation and glide of  $\frac{1}{2}\langle 1\ 1\ 0 \rangle$  dislocation on  $(1\ 0\ 0)_T$  plane. In addition, dislocations are deposited on ITBs in all cases after a dislocation loops a 3D twin. This is different from CTBs where defects are free in most cases. Therefore, ITBs may contribute more to work hardening than CTBs.

**Authorship contributions**

Yanxiang Liang: Investigation, Visualization, Formal analysis, Data curation, Writing - original draft.

Xiaofang Yang: Writing - review & editing, Funding acquisition.

Mingyu Gong: Methodology, Writing - review & editing.

Guisen Liu: Writing - review & editing.

Qing Liu: Funding acquisition, Project administration.

Jian Wang: Software, Supervision, Conceptualization, Writing - review & editing.

**Acknowledgments** — This research is funded by the National Natural Science Foundation of China (Grant No.51571046, No. 51421001), and the Project No. 2018CDJDCL0019 supported by the Fundamental Research Funds for the Central Universities. Thanks to the support of the 111 Project (B16007) by the Ministry of Education and the State Administration of Foreign Experts Affairs of China. Atomistic simulations were conducted at the Holland Computing Center (HCC), which is a high performance computing resource for the University of Nebraska System.

**References**

- [1] S. Tamura, The formation of twinned metallic crystals, *Proc. R. Soc. Lond. A* 113 (1926) 161–182, doi 10.1098/rspa.1926.0144
- [2] W. Burgers, Crystal growth in the solid state (recrystallization), *Physica* 15 (1949) 92–106, doi 10.1016/0031-8914(49)90031-2
- [3] S. Dash, N. Brown, An investigation of the origin and growth of annealing twins, *Acta Metall.* 11 (1963) 1067–1075, doi 10.1016/0001-6160(63) 90195-0
- [4] M.A. Meyers, L.E. Murr, A model for the formation of annealing twins in F.C.C. metals and alloys, *Acta Metall.* 26 (1978) 951–962.
- [5] M. Kumar, A.J. Schwartz, W.E. King, Microstructural evolution during grain boundary engineering of low to medium stacking fault energy fcc materials, *Acta Mater.* 50 (2002) 2599–2612, doi 10.1016/S1359-6454(02)00090-3
- [6] H. Gleiter, The formation of annealing twins, *Acta Metall.* 17 (1969) 1421–1428, doi 10.1016/0001-6160(69)90004-2
- [7] R. Fullman, J. Fisher, Formation of annealing twins during grain growth, *J. Appl. Phys.* 22 (1951) 1350–1355, doi 10.1063/1.1699865
- [8] Z. Wang, H. Margolin, Mechanism for the formation of high cycle fatigue cracks at fee annealing twin boundaries, *Metall. Trans. A* 16 (1985) 873–880, doi 10.1007/BF02814838
- [9] D. Vaughan, Annealing twin interfaces in an austenitic stainless steel, *Phil. Mag.* 22 (1970) 1003–1011, doi 10.1080/14786437008221070
- [10] M. Koyama, T. Sawaguchi, K. Tsuzaki, Quasi-cleavage fracture along annealing twin boundaries in a Fe–Mn–C austenitic steel, *ISIJ Int.* 52 (2012) 161–163, doi 10.2355/isijinternational.52.161
- [11] C. Pande, B. Rath, M. Imam, Effect of annealing twins on Hall-Petch relation in polycrystalline materials, *Mater. Sci. Eng. A* 367 (2004) 171–175, doi 10.1016/j.msea.2003.09.100



- [12] J.P. Hirth, J. Lothe, *Theory of Dislocations*, McGraw-Hill, New York, 1967.
- [13] Y. Zhang, T.T. Zuo, Z. Tang, M.C. Gao, K.A. Dahmen, P.K. Liaw, Z.P. Lu, Microstructures and properties of high-entropy alloys, *Prog. Mater Sci.* 61 (2014) 1–93, doi 10.1016/j.pmatsci.2013.10.001
- [14] D.B. Miracle, O.N. Senkov, A critical review of high entropy alloys and related concepts, *Acta Mater.* 122 (2017) 448–511, doi 10.1016/j.actamat.2016.08.081
- [15] K. Ming, X. Bi, J. Wang, Strength and ductility of CrFeCoNiMo alloy with hierarchical microstructures, *Int. J. Plast.* 113 (2019) 255–268, doi 10.1016/j.ijplas.2018.10.005
- [16] J. Wang, N. Li, O. Anderoglu, X. Zhang, A. Misra, J.Y. Huang, J.P. Hirth, Detwinning mechanisms for growth twins in face-centered cubic metals, *Acta Mater.* 58 (2010) 2262–2270, doi 10.1016/j.actamat.2009.12.013
- [17] J. Wang, N. Li, A. Misra, *Phil. Mag.* 93 (2013) 315–327, doi 10.1080/14786435.2012.716908
- [18] Z.H. Jin, P. Gumbsch, K. Albe, E. Ma, K. Lu, H. Gleiter, H. Hahn, Interactions between non-screw lattice dislocations and coherent twin boundaries in face-centered cubic metals, *Acta Mater.* 56 (2008) 1126–1135, doi 10.1016/j.actamat.2007.11.020
- [19] Z.H. Jin, P. Gumbsch, E. Ma, K. Albe, K. Lu, H. Hahn, H. Gleiter, The interaction mechanism of screw dislocations with coherent twin boundaries in different face-centred cubic metals, *Scr. Mater.* 54 (2006) 1163–1168, doi 10.1016/j.scriptamat.2005.11.072
- [20] M. Chassagne, M. Legros, D. Rodney, Atomic-scale simulation of screw dislocation/ coherent twin boundary interaction in Al, Au, Cu and Ni, *Acta Mater.* 59 (2011) 1456–1463, doi 10.1016/j.actamat.2010.11.007
- [21] Y.T. Zhu, X.L. Wu, X.Z. Liao, J. Narayan, L.J. Kecskés, S.N. Mathaudhu, Dislocation–twin interactions in nanocrystalline fcc metals, *Acta Mater.* 59 (2011) 812–821, doi 10.1016/j.actamat.2010.10.028
- [22] M. Sennour, S. Lartigue-Korinek, Y. Champion, M.J. Hytch, HRTEM study of defects in twin boundaries of ultra-fine grained copper, *Phil. Mag.* 87 (2007) 1465–1486, doi 10.1080/14786430601021611
- [23] I.J. Beyerlein, X. Zhang, A. Misra, Growth twins and deformation twins in metals, *Annu. Rev. Mater. Res.* 44 (2014) 329–363, doi 10.1146/annurevmatsci-070813-113304
- [24] Z. Wu, Y. Zhang, D. Srolovitz, Dislocation–twin interaction mechanisms for ultrahigh strength and ductility in nanotwinned metals, *Acta Mater.* 57 (2009) 4508–4518, doi 10.1016/j.actamat.2009.06.015
- [25] Q. Fang, F. Sansoz, Influence of intrinsic kink-like defects on screw dislocation– coherent twin boundary interactions in copper, *Acta Mater.* 123 (2017) 383–393, doi 10.1016/j.actamat.2016.10.032
- [26] J. Wang, H.C. Huang, Novel deformation mechanism of twinned nanowires, *Appl. Phys. Lett.* 88 (2006) 203112, doi 10.1063/1.2204760
- [27] N. Li, J. Wang, A. Misra, X. Zhang, J.Y. Huang, J.P. Hirth, Twinning dislocation multiplication at a coherent twin boundary, *Acta Mater.* 59 (2011) 5989–5996, doi 10.1016/j.actamat.2011.06.007

- [28] J. Wang, O. Anderoglu, J. Hirth, A. Misra, X. Zhang, Dislocation structures of  $\Sigma 3$  {112} twin boundaries in face centered cubic metals, *Appl. Phys. Lett.* 95 (2009) 021908, doi 10.1063/1.3176979
- [29] J. Wang, A. Misra, J.P. Hirth, Shear response of  $\Sigma 3$  {112} twin boundaries in face-centered-cubic metals, *Phys. Rev. B.* 83 (2011) 064106, doi 10.1103/PhysRevB.83.064106
- [30] J. Rittner, D. Seidman, K. Merkle, Grain-boundary dissociation by the emission of stacking faults, *Phys. Rev. B.* 53 (1996) R4241, doi 10.1103/PhysRevB.53.R4241
- [31] N. Li, J. Wang, J. Huang, A. Misra, X. Zhang, Influence of slip transmission on the migration of incoherent twin boundaries in epitaxial nanotwinned Cu, *Scr. Mater.* 64 (2011) 149–152, doi 10.1016/j.scriptamat.2010.09.031
- [32] Y. Liu, J. Jian, Y. Chen, H. Wang, X. Zhang, Plasticity and ultra-low stress induced twin boundary migration in nanotwinned Cu by in situ nanoindentation studies, *Appl. Phys. Lett.* 104 (2014) 231910, doi 10.1063/1.4882242
- [33] D. Bufford, Y. Liu, J. Wang, H. Wang, X. Zhang, In situ nanoindentation study on plasticity and work hardening in aluminium with incoherent twin boundaries, *Nat. Commun.* 5 (2014) 4864, doi 10.1038/ncomms5864
- [34] H. Van Swygenhoven, P.M. Derlet, A. Frøseth, Stacking fault energies and slip in nanocrystalline metals, *Nat. Mater.* 3 (2004) 399, doi 10.1038/nmat1136.
- [35] D. Barnett, J. Lothe, An image force theorem for dislocations in anisotropic bicrystals, *J. Phys. F: Metal Phys.* 4 (1974) 1618, doi 10.1088/0305-4608/4/10/010
- [36] Y. Mishin, M.J. Mehl, D.A. Papaconstantopoulos, A.F. Voter, J.D. Kress, Structural stability and lattice defects in copper: Ab initio, tight-binding, and embedded-atom calculations, *Phys. Rev. B.* 63 (2001) 224106, doi 10.1103/PhysRevB.63.224106
- [37] Y. Mishin, D. Farkas, M.J. Mehl, D.A. Papaconstantopoulos, Interatomic potentials for monoatomic metals from experimental data and ab initio calculations, *Phys. Rev. B.* 59 (1999) 3393–3407, doi 10.1103/PhysRevB.59.3393
- [38] H.P. Karnthaler, The study of glide on {001} planes in fcc metals deformed at room temperature, *Philos. Mag. A* 38 (1978) 141–156, doi 10.1080/01418617808239225
- [39] A. Korner, H. Karnthaler, The study of glide dislocation loops on {001} planes in a fcc alloy, *Philos. Mag. A* 42 (1980) 753–762, doi 10.1080/01418618008239382